JOURNAL OF MATERIALS SCIENCE 31 (1996) 3805–3812

Magnetic properties and thermal stability of Co–TM–Zr (TM=Nb, Ta, Mo, W, and Ni) amorphous sputtered films for magnetic heads

SHIGEKAZU OTOMO
Central Research Laboratory, Hitachi Ltd., Kokubunji, Tokyo 185, Japan

The magnetic properties and thermal stability Co–TM–Zr (TM = Nb, Ta, Mo, W, and Ni) amorphous films prepared by rf diode sputtering are investigated. Amorphous films with a homogeneous structure and coercive force H_c of less than 20 A m^{-1} are obtained at an argon gas pressure of 0.3–1 Pa. The formation range of the amorphous films is broad in the systems containing Ta and Nb, whereas it is limited to the composition range greater than 4–5 at % of Zr in the systems of Mo, W, and Ni. The magnetostriction λ_s depends on the concentration ratio of Zr and the TM. Films with zero λ_s are obtained at concentration ratios C_{Zr}/C_{TM} ranging from 0.3 for Co–Nb–Zr films to 1.5 – 1.7 for Co–W–Zr films. The crystallization temperature T_x is highest in Co–Ta–Zr films and lowest in Co–Mo–Zr films when λ_s is zero and both films have the same saturation magnetic flux density B_s. The anisotropy field H_k is highest in Co–Ni–Zr films and lowest in Co–Nb–Zr films. These results indicate that Co–Ta–Zr and Co–Nb–Zr amorphous films are suitable for use as magnetic head materials because of the Co–Ta–Zr film's high T_x and B_s, and the Co – Nb – Zr film's small λ_s and low H_k.

1. Introduction

Amorphous alloys have been prepared by various techniques such as rapid quenching or sputtering. Sputtering is generally considered to be the best technique since amorphous alloys with wide composition ranges can be easily prepared even when using oxizable materials or those with high melting temperatures. The demand for amorphous alloys in thin film form has increased greatly since the development of thin film magnetic devices. Therefore, much work has been recently performed on amorphous alloy films prepared by sputtering. Amongst these alloys, metal–metal type amorphous alloys which consist of Co and IIIa–VIa transition metals show good corrosion resistance and thermal stability compared to the conventional metal–metalloid type amorphous alloys [1, 2]. Furthermore, the eddy current loss in metal–metal type amorphous alloys is lower than in crystalline magnetic alloys because of their high electrical resistivity ρ. Therefore, metal–metal amorphous alloy films are considered promising for use as magnetic materials for thin film magnetic heads or video heads.

In order to apply amorphous alloys in magnetic heads, a high saturation magnetic flux density B_s, a low coercive force H_c and a high permeability μ are needed to obtain good recording and reproducing characteristics. Also a high thermal stability is required to prevent crystallization of the amorphous alloys during heat treatment in the head fabrication process. Furthermore, it is necessary that the magnetostriction λ_s be close to zero in order to prevent degradation of soft magnetic properties by stress during the head fabrication. In Co-based metal–metal amorphous alloys, Y, Ti, Zr, and Hf help to shift λ_s to positive values and Nb, Ta, Mo, and Ni help to shift it to negative values [3–5]. Therefore, ternary amorphous alloy systems have been investigated because a zero λ_s can be obtained by controlling the concentration ratio of these two kinds of elements [1, 5, 6]. However, there are few reported papers in which the magnetic properties of these ternary amorphous alloy systems are compared.

In this work, Co–TM–Zr (TM = Nb, Ta, Mo, W, and Ni) amorphous films were prepared by sputtering, and their magnetic properties and thermal stability were investigated to find out which amorphous alloy films are most suitable for magnetic heads.

2. Experimental procedures

A conventional rf diode sputtering apparatus with composite targets of a Co disk (150 mm in diameter) and small plates of the TM and Zr were used for the film preparation. The composition of the films was controlled by varying the area of the small plates.

After evacuating the sputtering chamber to below 1×10^{-4} Pa, argon gas of 99.99% purity was introduced into the chamber and pre-sputtering was performed for about 60 min. Then films about 2 μm thick were deposited on crystallized glass substrates (10 mm in diameter and 0.5 mm thick) which were placed on a water-cooled substrate holder. The distance between the target and the substrates was 50 mm. As the

0022–2461

standard sputtering conditions, an input power density of 15.8 kW m^{-2}, an argon gas pressure of 0.7 Pa, and a deposition rate of about 17 nm per min were used.

The composition of the films was determined by inductively coupled argon plasma spectroscopy (ICPS) and the crystal structure was characterized by X-ray diffraction. The morphology of the films was observed with a scanning electron microscope (SEM). The saturation magnetic flux density B_s at room temperature was measured with a vibrating sample magnetometer (VSM) while applying a magnetic field of 8×10^5 A m^{-1}. The coercive force H_c and the anisotropy field H_k were measured with a B–H curve tracer at a frequency of 40 Hz. The relative permeability μ was measured with a vector impedance meter and a horseshoe-shaped ferrite core. The magnetostriction λ_s was obtained from the change in the anisotropy field H_k when the sample was bent [7]. The electrical resistivity ρ was measured using a four-terminal method. The crystallization temperature T_x of the films was determined by measuring of the temperature dependence of ρ [4].

3. Results and discussion

3.1. Dependence of magnetic properties on sputtering conditions

The effect of the sputtering conditions on the magnetic properties of the amorphous films were examined before the study on the effects of the composition. A $Co_{80}Mo_{11.5}Zr_{8.5}$ alloy is used in this experiment because this alloy is known to be easily made amorphous by the rapid quenching technique [1].

Fig. 1 shows the change in coercive force H_c of $Co_{80}Mo_{11.5}Zr_{8.5}$ sputtered films as a function of argon gas pressure P_{Ar}. All the films deposited at various

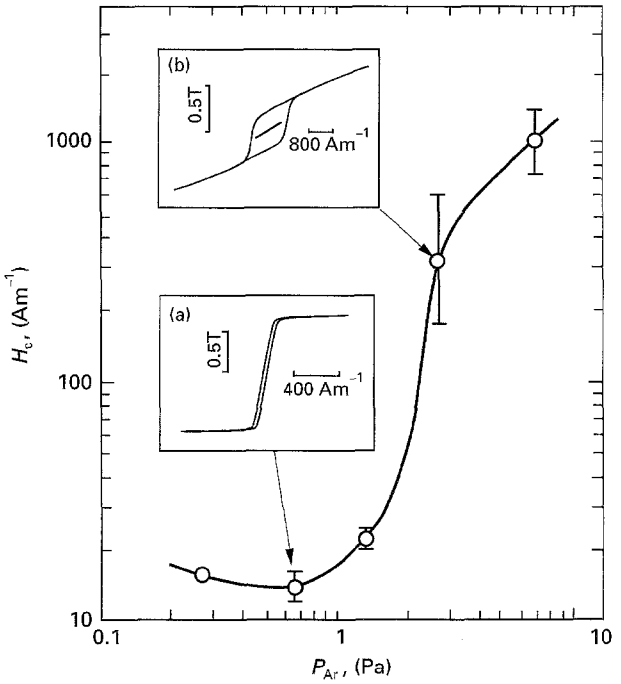

Figure 1 Change in coercive force H_c of $Co_{80}Mo_{11.5}Zr_{8.5}$ sputtered films as a function of argon gas pressure P_{Ar}.

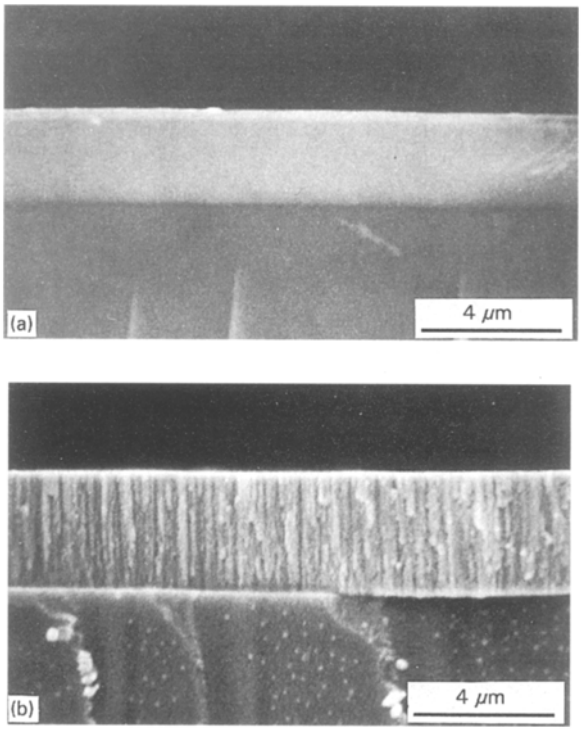

Figure 2 Scanning electron micrographs of the cross-sections of $Co_{80}Mo_{11.5}Zr_{8.5}$ amorphous films deposited at P_{Ar} of (a) 0.7 Pa and (b) 7 Pa.

P_{Ar} are amorphous, showing no crystalline peaks in the X-ray diffraction patterns. Amorphous films with low H_c, under 20 A m^{-1}, are obtained at P_{Ar} less than 1 Pa. On the other hand, H_c rises quickly for films deposited at P_{Ar} higher than 1 Pa.

Fig. 2 shows scanning electron micrographs of cross-sections of the films deposited at P_{Ar} of 0.7 and 7 Pa. Although the film deposited at 0.7 Pa has a homogeneous structure, the film deposited at 7 Pa exhibits a heterogeneous columnar structure. The columnar structure is known to yield a large magnetic anisotropy perpendicular to the film surface, and this anisotropy gives rise to a stripe domain structure which produces a B–H curve such as that shown in Fig. 1b [8, 9]. Therefore, the high H_c of films deposited at high P_{Ar} is attributed to the columnar structure. In this work, all amorphous films discussed in the following sections were deposited at a P_{Ar} of 0.7 Pa.

3.2. Properties of Co–Nb–Zr amorphous films

It has been reported that Zr has one of the highest levels of glass formability of all the transition metals and that Nb has a high level of glass formability as compared to other elements with a negative contribution to λ_s [5]. Thus, a Co–Nb–Zr system appears likely to have a broad range of compositions where the amorphous phase forms.

Fig. 3 shows the dependence of saturation magnetic flux density B_s, coercive force H_c, and electrical resistivity ρ on concentration x for $Co_{1-x}(Nb, Zr)_x$ sputtered films, in which the concentration ratio C_{Zr}/C_{Nb} is 0.75. In the area of low x, the sputtered films are shown to be crystalline by the crystalline peaks in

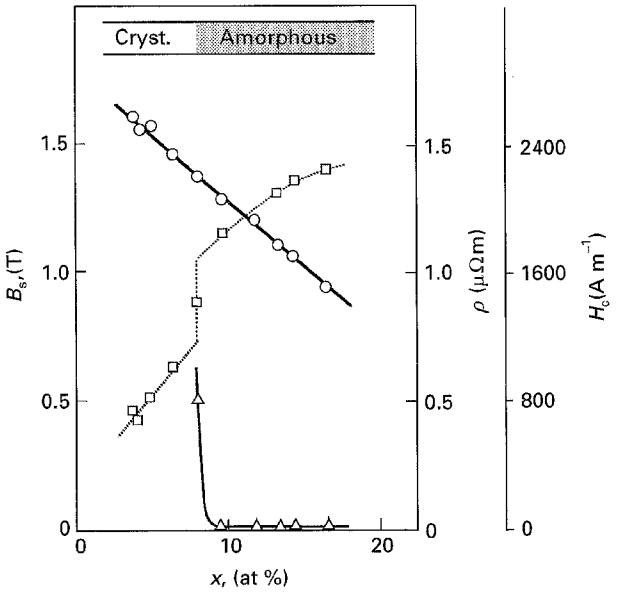

Figure 3 The dependence of saturation magnetic flux density B_s (○), coercive force H_c (△) and electrical resistivity ρ (□) on concentration x for $Co_{1-x}(Nb, Zr)_x$ sputtered films, in which the concentration ratio C_{Zr}/C_{Nb} is 0.75.

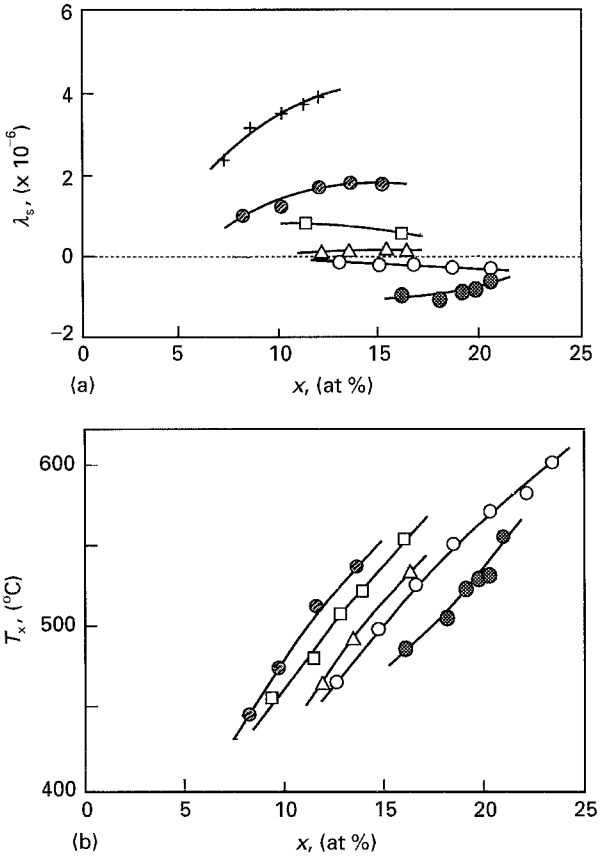

Figure 4 The change of (a) magnetostriction λ_s and (b) crystallization temperature T_x with concentration x and concentration ratio C_{Zr}/C_{Nb} for Co–Nb–Zr amorphous films. Data are reported for the end compositions; (+) Co_{100-x} Zr_x and (●) $Co_{100-x}Nb_x$. The intermediate compositions $Co_{100-x}(NbZr)_x$ are represented by the ratio C_{Zr}/C_{Nb} values of; (◉) 2, (□) 0.75, (△) 0.4 and (○) 0.25.

their X-ray diffraction pattern. These films have a H_c greater than 800 A m^{-1}. When the concentration x is increased to above 8 at %, the films become amorphous and show no crystalline peaks in their X-ray diffraction pattern. At this point, H_c abruptly decreases to less than 20 A m^{-1}. The electrical resistivity ρ increases with increasing x, and shows a jump at the phase shift from crystalline to amorphous phases. On the other hand, the saturation flux density B_s continuously decreases with increasing x even at the boundary between crystalline and amorphous phases.

Fig. 4a shows the change of magnetostriction λ_s with the concentration x and the concentration ratio C_{Zr}/C_{Nb}. The magnetostriction λ_s is 2×10^{-6}–4×10^{-6} for the Co–Zr amorphous films, and about -1×10^{-6} for the Co–Nb films, which are consistent with the reported values [2, 3]. For Co–Nb–Zr films, λ_s shows intermediate values between those of the Co–Zr and Co–Nb films; a zero λ_s is obtained at the concentration ratio C_{Zr}/C_{Nb} of about 0.3.

The crystallization temperature T_x increases with increasing x as shown in Fig. 4b. Further, the films with high C_{Zr}/C_{Nb} show high T_x because the glass formability of Zr is higher than that of Nb [5].

Fig. 5 is a triangular diagram showing the formation range of the amorphous phase together with the composition dependence of B_s, T_x, and λ_s for the ternary Co–Nb–Zr alloy system. The amorphous phase is obtained at compositions higher than 6 at % Zr and 17 at % Nb for Co–Zr and Co–Nb alloy films, respectively. In a Co–Nb–Zr system, the boundary between amorphous and crystalline phases is located on the line connecting these points. The saturation magnetic flux density B_s continuously increases with the concentration of Co. The line of zero λ_s is located at the concentration ratio C_{Zr}/C_{Nb} of about 0.3. The composition range with small $|\lambda_s|$ of less than 1×10^{-6} for the Co–Nb–Zr system is considerably broader than that for the other amorphous or crystalline magnetic alloys because the original absolute values of λ_s in the Co–Zr and Co–Nb films are small. This feature is extremely desirable for magnetic head materials produced by sputtering, a process in which it is rather difficult to control compositions.

3.3. Properties of Co–TM–Zr amorphous alloy films

Fig. 6 shows the formation ranges of the amorphous phase and the composition dependencies of B_s, T_x, and λ_s for Co–Ta–Zr, Co–Mo–Zr, Co–W–Zr, and Co–Ni–Zr systems. In systems containing Ta and Nb, which both have high glass formability amongst transition metals, the formation range of the amorphous phase extends to the low concentration of Zr, whereas it is limited to the composition range higher than about 5 at % Zr in the systems containing Mo, W, and Ni which have low glass formability.

The saturation magnetic flux density B_s continuously increases with increasing Co concentration except in the Co–Ni–Zr films, and tends to decrease in the composition region of low C_{Zr}/C_{TM} in the systems containing Mo and W. For Co–Ni–Zr films, B_s tends to increase with the sum of the Co and Ni concentrations due to the magnetic moment of Ni.

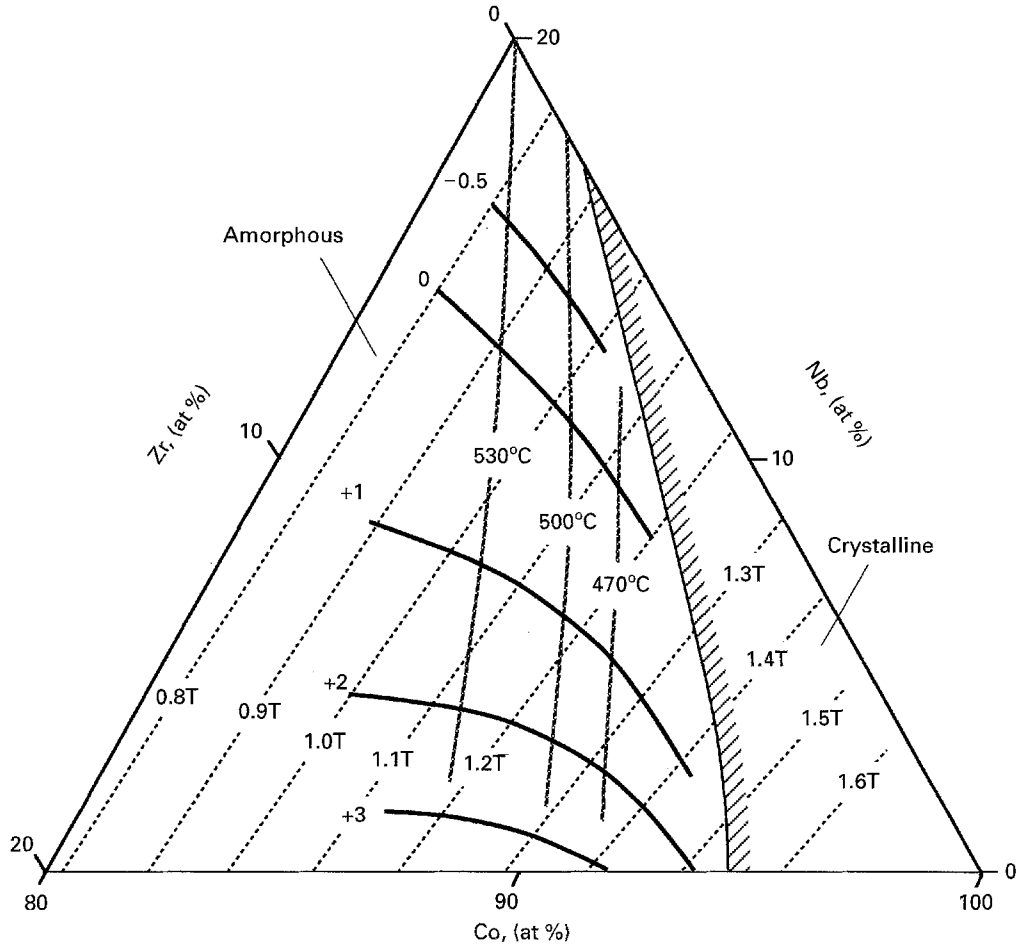

Figure 5 Formation range of amorphous phase and composition dependence of (– –) B_s, (- - -) T_x, and (—) $\lambda_s \times 10^{-6}$ for a ternary Co–Nb–Zr alloy system.

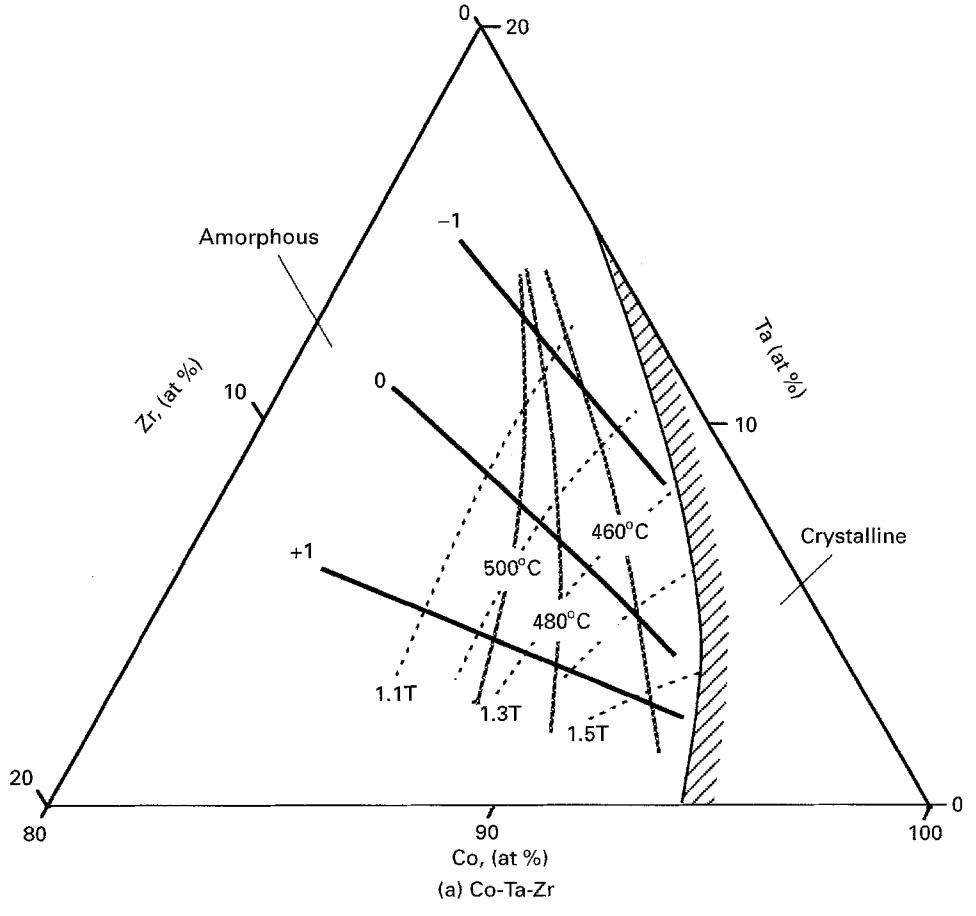

Figure 6 Formation ranges of amorphous phase and composition dependencies of (– –) B_s, (- - -) T_x, and λ_s ($\times 10^{-6}$) for ternary (a) Co–Ta–Zr, (b) Co–Mo–Zr, (c) Co–W–Zr, and (d) Co–Ni–Zr alloy systems.

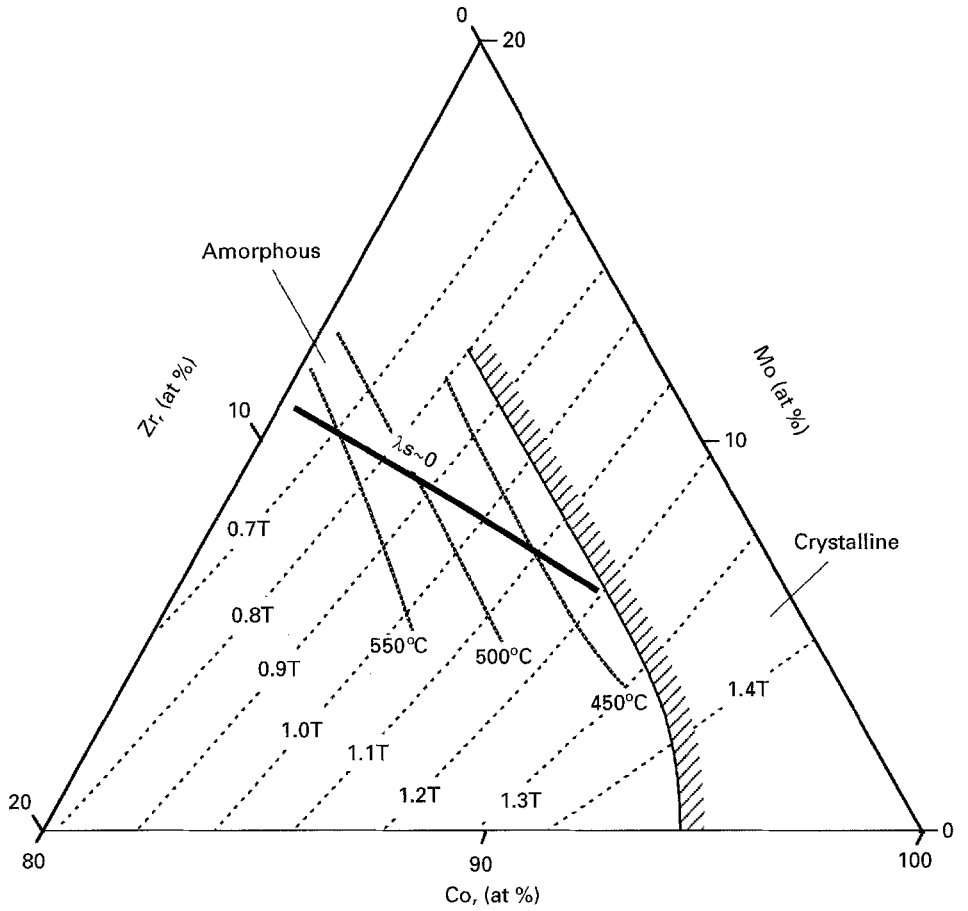

(b) Co-Mo-Zr

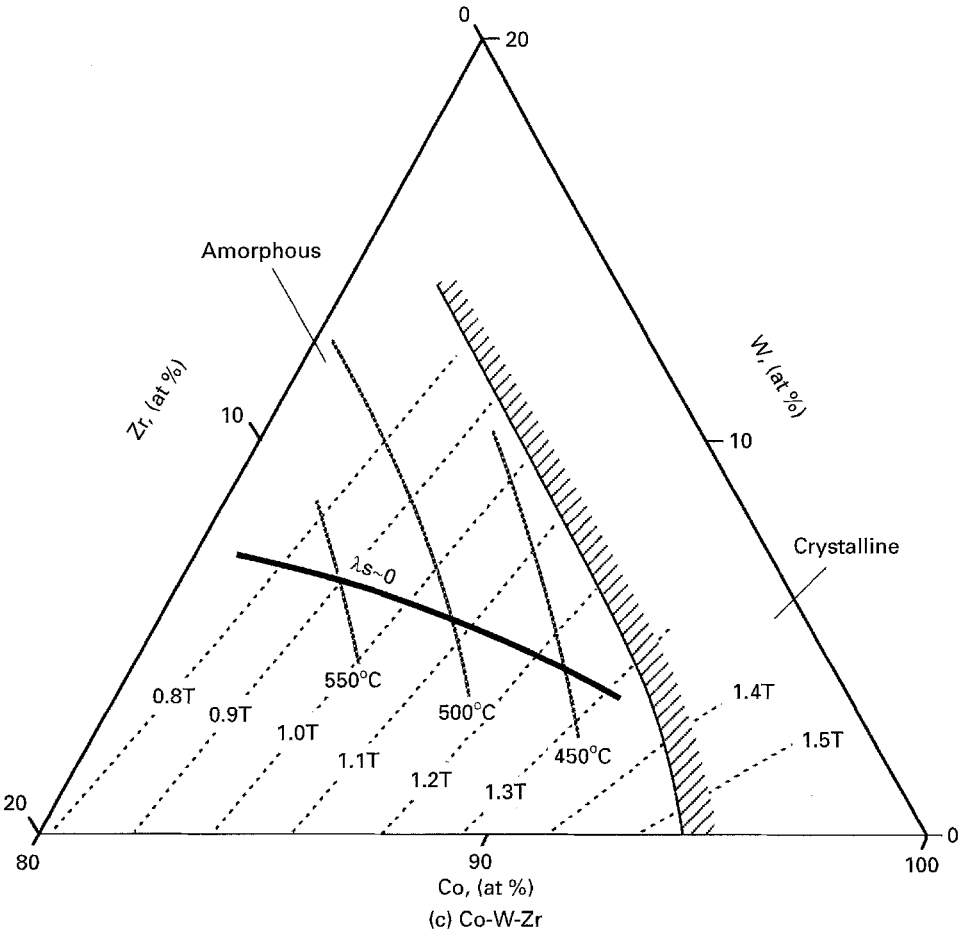

(c) Co-W-Zr

Figure 6 Continued.

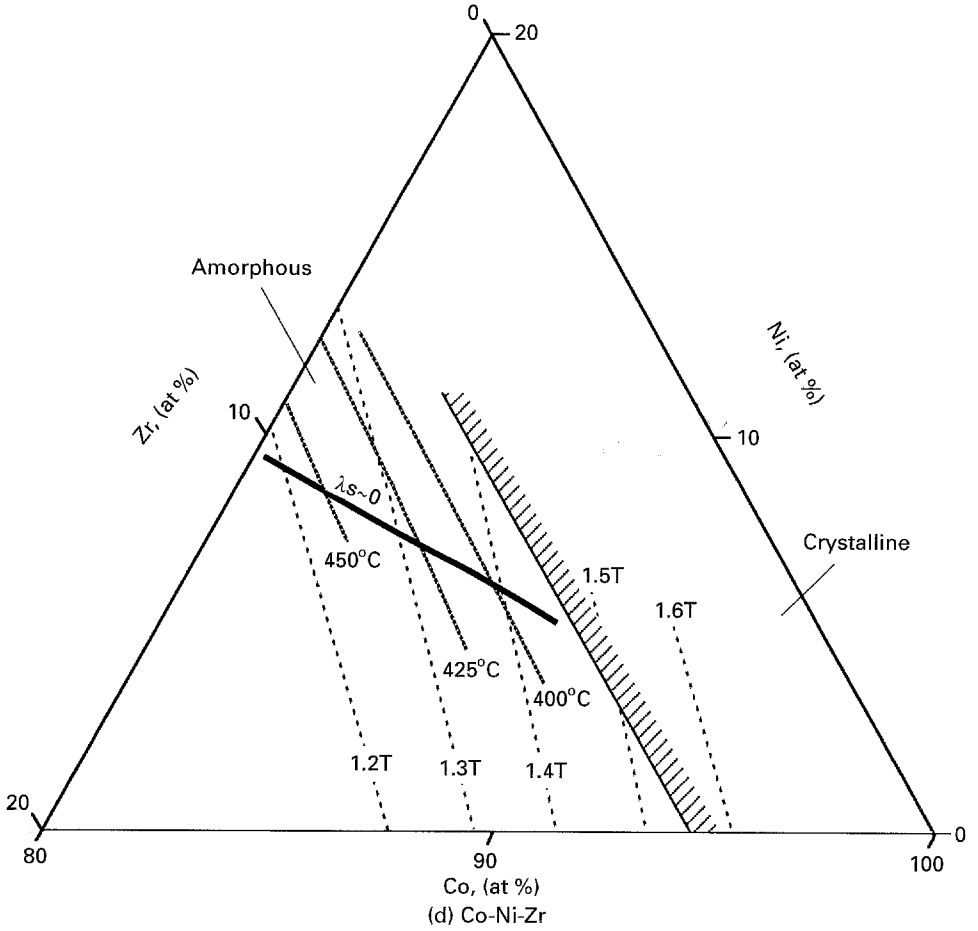

Figure 6 Continued.

The magnetostriction constant λ_s depends on the concentration ratio of Zr, which contributes positively to λ_s, and TM which contributes negatively. Films with zero λ_s are obtained at a low concentration ratio C_{Zr}/C_{Nb} of 0.3 for Co–Nb–Zr films because of the small effect Nb has on λ_s. As the effect of TM on λ_s increases, the concentration ratio C_{Zr}/C_{TM} for zero λ_s becomes higher: for example C_{Zr}/C_{TM} of 0.7–0.8 for Co–Ta–Zr or Co–Mo–Zr, 1.1 for Co–Ni–Zr, and 1.5–1.7 for Co–W–Zr.

To compare the properties of amorphous films used as magnetic head materials, the films must be compared at the same λ_s. Fig. 7 shows the relation between the crystallization temperature T_x and the saturation magnetic flux density B_s when λ_s is zero. The crystallization temperature T_x decreases with increasing B_s while the concentration of Co increases. When T_x is compared amongst films with the same B_s, T_x is highest in the system containing Ta, which has high glass formability, and lowest in the system containing Mo which has low glass formability. The B_s of Co–Ta–Zr films is 0.4 T higher than that of Co–Mo–Zr films when films with the same T_x are compared. Therefore, Co–Ta–Zr amorphous films are best suited to the demand for high thermal stability and high B_s.

The maximum B_s of amorphous films with zero λ_s is also shown in Fig. 7. The maximum B_s is also highest in Co–Ta–Zr films and lowest in Co–Mo–Zr films. However, the maximum B_s and T_x for Co–Nb–Zr films are both lower than those for Co–W–Zr films,

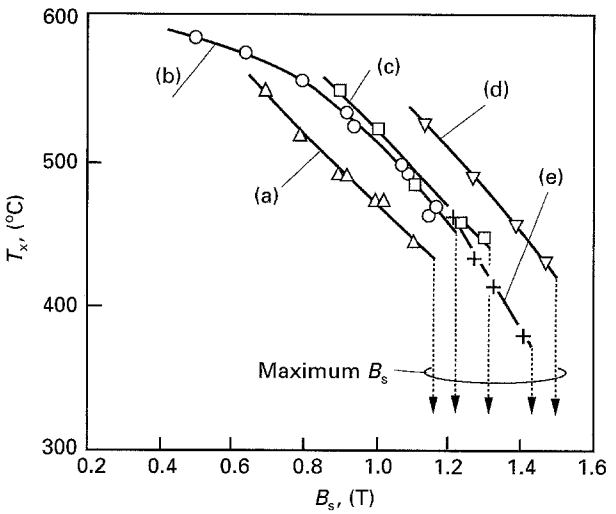

Figure 7 Relation between crystallization temperature T_x and saturation magnetic flux density B_s when λ_s is zero for (a) Co–Mo–Zr, (b) Co–Nb–Zr, (c) Co–W–Zr, (d) Co–Ta–Zr and (e) Co–Ni–Zr.

although the glass formability of Nb is higher than that of W. This is due to the higher concentration ratio C_{Zr}/C_{TM} for zero λ_s in Co–W–Zr than in Co–Nb–Zr and to the high glass formability of Zr. Therefore, T_x and the maximum B_s when λ_s is zero depend not only on the glass formability of TM but also on the concentration ratio C_{Zr}/C_{TM} for zero λ_s.

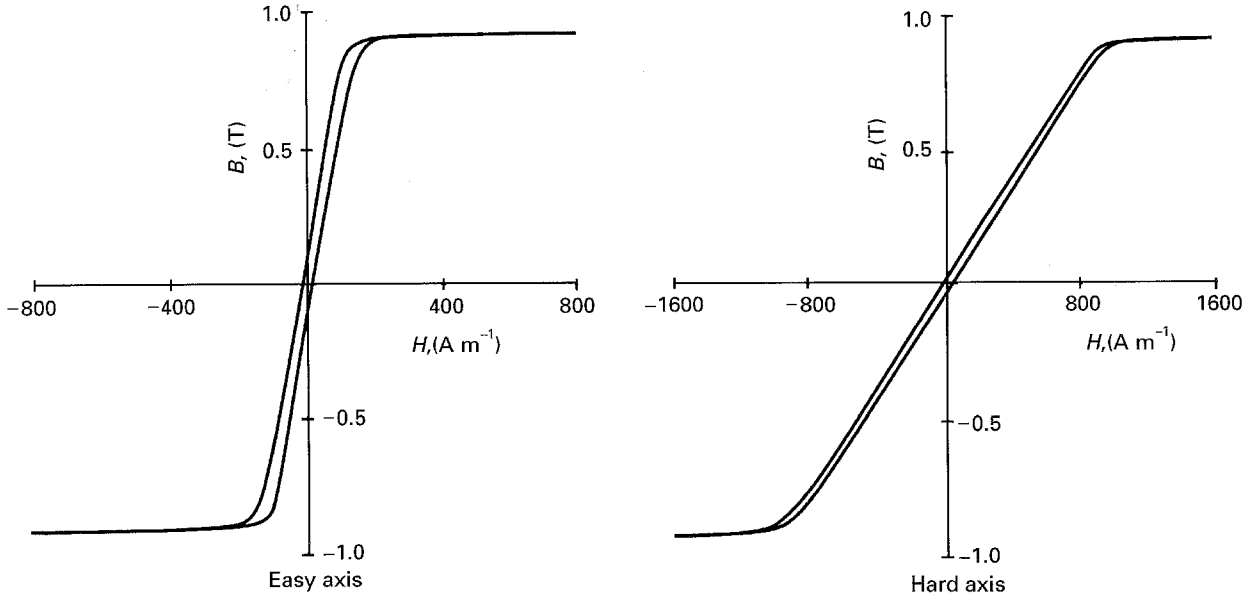

Figure 8 B–H loops for $Co_{84}Nb_{13}Zr_3$ amorphous film.

3.4. Compositional dependence of induced anisotropy

The amorphous films prepared in this work have a typical uniaxial magnetic anisotropy whose easy axis is in the plane of the films, as is shown in Fig. 8. In these magnetic films, permeability is generally low in the easy direction because magnetization changes are caused by wall motion which hardly occurs in a low field below H_c. On the other hand, permeability is high in the hard direction because of the magnetization changes caused by the rotation of the magnetic moment which occurs easily even in a low field.

In the films with uniaxial anisotropy, permeability μ in the hard direction approximately equal the ratio $B_s/(\mu_o H_k)$, where μ_o is the permeability of a vacuum and H_k is the anisotropy field. Therefore, a high B_s and a low H_k are needed to obtain high permeability films. Fig. 9 shows the relation between the anisotropy fields H_k and the saturation magnetic flux density B_s when λ_s is zero. The anisotropy field H_k is quite low when B_s is less than 0.5 T, and then increases with B_s when B_s is higher than 0.5 T; the Co–Ni–Zr films are an exception, however. The dotted lines in Fig. 9 also show the permeability μ obtained from the ratio $B_s/(\mu_0 H_k)$. It can be seen that the permeability μ is reduced by increasing B_s causing a rapid increase of H_k.

As shown in Fig. 9, the strength of the anisotropy field H_k decreases in the order of Co–Ta–Zr, Co–W–Zr, Co–Mo–Zr and Co–Nb–Zr. Co–Ni–Zr amorphous films have the highest anisotropy field H_k, however, and their dependency of H_k on B_s is quite different from that of the other amorphous films.

It has been pointed out that directional pair ordering is responsible for induced anisotropy in amorphous alloys containing two species of magnetic atoms [10, 11]. In amorphous alloys which contain only one species of magnetic atoms, the induced anisotropy has been understood using the framework of the pair-ordering model assuming a pseudo-dipole interaction

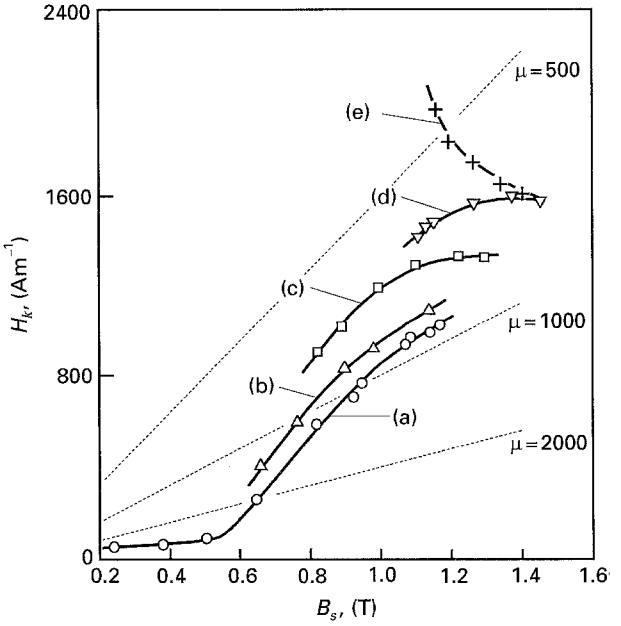

Figure 9 Relation between anisotropy field H_k and saturation magnetic flux density B_s when λ_s is zero for (a) Co–Nb–Zr, (b) Co–Mo–Zr, (c) Co–W–Zr, (d) Co–Ta–Zr and (e) Co–Ni–Zr.

between a magnetic atom pair [11]. The high anisotropy field H_k in Co–Ni–Zr films shown in Fig. 9 is attributable to the directional pair ordering of nickel and cobalt atoms adding to the pseudo-dipole interaction between a cobalt atom pair [12]. On the other hand, the dependencies of H_k on B_s and on the element TM in Co–TM–Zr (TM = Nb, Ta, Mo, and W) films can be attributed to the change in the magnetic moment of the cobalt atom which affects the pseudo-dipole interaction [11].

The magnitude of the induced anisotropy in amorphous alloys can be controlled by a magnetic anneal after film preparation. However, it is difficult to control anisotropy when the amorphous films are used in heads. Therefore, amorphous films such as

Co–Nb–Zr films with small anisotropy will be useful for magnetic heads.

4. Conclusions

Co–TM–Zr (TM = Nb, Ta, Mo, W, and Ni) amorphous films were prepared by conventional rf diode sputtering, and their magnetic and thermal properties were investigated. The results are as follows:

(1) Amorphous films with a homogeneous structure and H_c of less than 20 A m^{-1} were obtained at an argon gas pressure of 0.3–1 Pa.

(2) The formation range of the amorphous phase is broad in the systems containing Ta and Nb, which have a high glass formability, whereas the range is limited to the composition range greater than 4–5 at% of Zr in the systems of Mo, W, and Ni that have low glass formability.

(3) Films with zero magnetostriction λ_s are obtained at the concentration ratio C_{Zr}/C_{TM} of 0.3 for Co–Nb–Zr, 0.7–0.8 for Co–Ta–Zr and Co–Mo–Zr, 1.1 for Co–Ni–Zr, and 1.5–1.7 for Co–W–Zr films. Amongst these amorphous films, the composition range with small $|\lambda_s|$ is broadest for Co–Nb–Zr films.

(4) The crystallization temperature T_x of the films decreases in the order of Co–Ta–Zr, Co–W–Zr, Co–Ni–Zr, Co–Nb–Zr and Co–Mo–Zr when λ_s is zero and the films have the same saturation flux density B_s. This order of decreasing T_x depends on the glass formability of the TM and the concentration ratio C_{Zr}/C_{TM} at zero λ_s.

(5) The anisotropy field H_k decreases in the order of Co–Ni–Zr, Co–Ta–Zr, Co–W–Zr, Co–Mo–Zr, and Co–Nb–Zr. The high H_k in Co–Ni–Zr films is attributable to the directional pair ordering of Ni and Co atoms.

(6) Consequently, Co–Ta-Zr amorphous films appear to be an excellent magnetic head material because of their high T_x and high B_s. On the other hand, Co–Nb–Zr amorphous films also appear excellent due to their small λ_s and low H_k.

Acknowledgement

I thank Mr. S. Kojima for his collaboration on the composition analysis and Mr. Y. Hamakawa for his help preparing the amorphous films. I am also grateful to Mr. N. Kumasaka, Mr. T. Yamashita, and Dr. M. Kudo for their helpful discussions and encouragement.

References

1. M. NOSE and J. KANEHIRA, *J. Appl. Phys.* **52** (1981) 1911.
2. M. NAKA, N. S. KAZAMA, H. FUJIMORI and T. MASUMOTO, In Proceedings 4th International Conference on Rapidly Quenched Metals, eds., T. Masumoto and K. Suzuki, Vol 2 (Japan Inst. Metals, Sendai, 1982) 919.
3. Y. SHIMADA and H. KOJIMA, *J. Appl. Phys.* **53** (1982) 3156.
4. M. NAOE, H. KAZAMA, Y. HOSHI and S. YAMANAKA, *ibid.* **53** (1982) 7846.
5. N. S. KAZAMA, H. FUJIMORI and K. HIROSE, *IEEE Trans. Magn.* **MAG-18** (1982) 1185.
6. Y. HOSHI, H. KAZAMA, M. NAOE and S. YAMANAKA, *ibid.* **MAG-19** (1983) 1958.
7. S. TSUNASHIMA, H. TAKAGI, K. KAMEGAKI, T. FUJII and S. UCHIYAMA, *ibid.* **MAG-14** (1978) 844.
8. H. FUJIWARA and Y. SUGITA. *ibid.* **MAG-4** (1968) 22.
9. N. SAITO, H. FUJIWARA and Y. SUGITA, *J. Phys. Soc. Jpn.* **19** (1964) 1116.
10. F. E. LUBORSKY and J. L. WALTER, *IEEE Trans. Magn.* **MAG-13** (1977) 953.
11. H. FUKUNAGA and K. NARITA, *Jpn. J. Appl. Phys.* **24** (1985) 24.
12. H. J. DE WIT, C. H. M. WITMER and F. W. A. DIRNE, *IEEE Trans. Magn.* **MAG-23** (1987) 2123.

Received 23 January 1995
and accepted 7 November 1995